Dalton
Transactions

Cite this: *Dalton Trans.*, 2011, **40**, 3128

www.rsc.org/dalton

PAPER

para-Benzene disulfonic acid and its tetrachloro and tetrafluoro derivatives—studies towards polyhalogenated metal–organic-frameworks with sulfo analogues of terephthalic acid†

Thomas W. T. Muesmann, Christina Zitzer, Andrea Mietrach, Thorsten Klüner, Jens Christoffers* and Mathias S. Wickleder*

Received 13th September 2010, Accepted 1st December 2010
DOI: 10.1039/c0dt01223h

We developed convenient synthetic routes for the preparation of *para*-benzene disulfonic acid (H_2BDS) and its tetrachloro (H_2BDSCl_4) and tetrafluoro (H_2BDSF_4) derivatives. The reaction of these acids with zinc nitrate in DMF led to single crystals of $[Zn(BDS)(DMF)_2]$ (triclinic, $P\bar{1}$, $Z = 2$, $a = 976.62(4)$, $b = 986.85(4)$, $c = 1014.40(4)$, $\alpha = 69.106(2)°$, $\beta = 68.746(2)°$, $\gamma = 86.295(2)°$, $wR_2 = 0.0627$), $[Zn(BDSCl_4)(DMF)_4]$ (triclinic, $P\bar{1}$, $Z = 1$, $a = 831.5(1)$, $b = 905.2(1)$, $c = 989.6(1)$, $\alpha = 90.44(2)°$, $\beta = 91.41\ (2)°$, $\gamma = 106.72(2)°$, $wR_2 = 0.0635$), and $[Zn(BDSF_4)(DMF)_4]$ (monoclinic, $P2_1/c$, $Z = 2$, $a = 889.01(3)$, $b = 968.91(3)$, $c = 1633.07(5)$ pm, $\beta = 106.524(2)°$, $wR_2 = 0.0948$). While $[Zn(BDS)(DMF)_2]$ exhibits a layer structure, the disulfonate linkers connect the zinc ions into chains in the crystal structures of $[Zn(BDSCl_4)(DMF)_4]$ and $[Zn(BDSF_4)(DMF)_4]$. Thermoanalytical investigations revealed that desolvation of the compounds occurs in a temperature range between 100 and 200 °C. The solvent free sulfonates show remarkably high stabilities, $[Zn(BDS)(DMF)_2]$ is stable up to nearly 600 °C. The halogenated acids were also used to prepare copper salts from aqueous solutions and $Cu_2(OH)_2(CO_3)$ (malachite) as a copper source. The crystal structure of $[Cu(H_2O)_6](BDSF_4)$ (triclinic, $P\bar{1}$, $Z = 1$, $a = 510.45(2)$, $b = 744.68(3)$, $c = 1077.77(4)$ pm, $\alpha = 85.627\ (2)°$, $\beta = 77.449\ (2)°$, $\gamma = 76.015\ (2)°$) exhibits complex cations and uncoordinated sulfonate anions, while in $[Cu(BDSCl_4)(H_2O)_4]$ (orthorhombic, $Pnma$, $Z = 4$, $a = 721.27(2)$, $b = 2147.81(6)$, $c = 979.42(3)$ pm) the Cu^{2+} ions are linked to infinite chains in the crystal structure. The most interesting structural feature of $[Cu(BDSCl_4)(H_2O)_4]$ is the significant deviation from planarity of the disulfonate dianion. Theoretical investigations revealed that a boat conformation is favoured due to steric hindrance in cases where a *syn* coordination of the sulfonate groups occurs. The thermal behaviour of the copper compounds was also investigated by DTA/TG measurements and X-ray powder diffraction.

Introduction

Materials with open framework structures consisting of metal centers as knots and organic linkers (so called metal–organic-frameworks) have entered the focus of interest due to their broad range of promising chemical and physical properties.[1] Carboxylates define a privileged class of anions used as linkers in MOFs, because they are readily available in a great variety at relatively low costs. The respective sulfo analogues of these acids are scarcely explored, even if their potential to act as suitable linkers for building MOFs has been mentioned occasionally.[2] This potential arises on one hand from the different coordination properties of sulfonate groups compared to those of carboxylate groups, and on the other hand from the higher thermal stability of sulfonates compared to carboxylates. Especially the latter point is of utmost importance with respect to the application of such compounds. For example, copper(II) terephthalate decomposes between 160–230 °C,[3] whereas copper(II) 1,4-benzenedisulfonate is stable up to 400 °C.[4] The main reason for our poor knowledge of polysulfonates as linkers is the limited availability of the respective acids. In particular, the analogues of those carboxylic acids that have been used with great success so far, *e.g.* terephthalic acid (**1**), trimesic acid (**2**), and pyromellitic acid (**3**), have no convenient routes for their multigram preparation starting from cheap materials (see Scheme 1 for structures). Providing effective syntheses as a key issue for the implementation of polysulfonate linkers in MOF chemistry was the driving force for us to initiate a research program on new oligosulfonic acids. In the course of these studies we have already developed scalable synthetic routes to 1,4-benzene disulfonic acid (**4**, H_2BDS),[4] 1,3,5-benzene

---

Institut für Reine und Angewandte Chemie, Carl von Ossietzky-Universität Oldenburg, D-26111, Oldenburg, Germany. E-mail: mathias.wickleder@uni-oldenburg.de; Fax: +49 441 798 3873

† CCDC reference numbers 763637, 763638, 763639, 776934, 776935, 777578. For crystallographic data in CIF or other electronic format see DOI: 10.1039/c0dt01223h

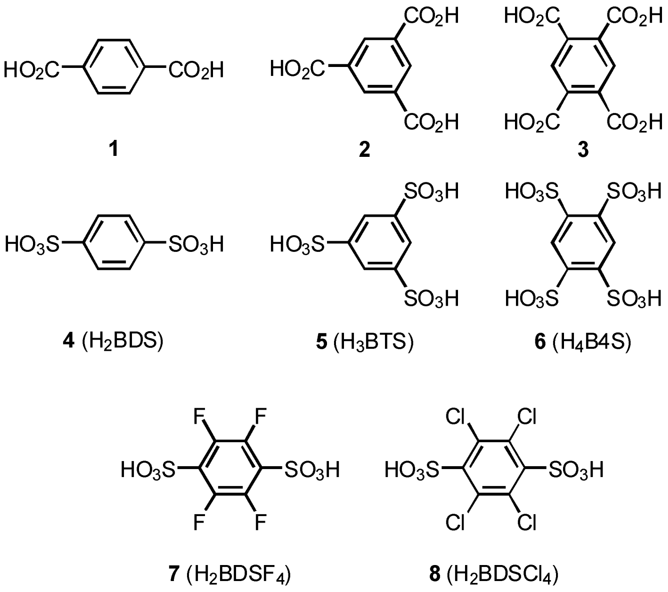

Scheme 1 Carboxylic and sulfonic acids as linker molecules for metal–organic-frameworks.

trisulfonic acid (**5**, H_3BTS),[4] and 1,2,4,5-benzene tetrasulfonic acid (**6**, H_4B4S)[5] as sulfo-analogues of terephthalic (**1**), trimesic (**2**), and pyromellitic acid (**3**). We furthermore were able to isolate and structurally characterize the copper(II) salts of all three sulfonic acids **4**–**6**. The most important result of these studies was—as already mentioned above—the increased thermal stability of such compounds compared to copper(II) carboxylates. We now report on the extension of our efforts by developing synthetic routes to the tetrafluoro- (**7**, H_2BDSF_4) and tetrachloro-derivatives (**8**, H_2BDSCl_4) of 1,4-benzene disulfonic acid (**4**). This study was clearly inspired by recent investigations of other groups on tetrafluoro-[6] and tetrachloroterephthalates[7] as linker molecules in MOFs. In particular, perfluorination might lead to enhanced hydrogen adsorption properties due to hydrophobation of internal surfaces of such frameworks.[6a]

Results

Organic Syntheses

Perfluorinated disulfonic acid H_2BDSF_4 (**7**) has previously been reported by Sartori and coworkers, who developed a three step synthesis from pentafluorobenzene, which was first monosulfonated in liquid SO_3.[8] The next step was a regioselective nucleophilic substitution with KHS. Finally, oxidation was achieved with chlorine in the presence of peracetic acid. In order to avoid operations with SO_3 and Cl_2, we were seeking for a preparative alternative for the introduction of sulfur groups at an aromatic ring. One generally useful reaction could be the intramolecular nucleophilic displacement of an C–O by an C–S bond in an aryl-thiocarbamate (so called Newman–Kwart[9] or Schönberg-rearrangement),[10] which would transform a phenol- into a thiophenol-derivative. Commercially available tetrafluorohydroquinone **9** was therefore esterified with an excess of thiocarbamoylchloride to yield the *O*-diester **10**, which was isolated in 73% yield after chromatography (Scheme 2). The rearrangement reaction proceeded in Ph_2O at 200 °C with 61% yield after chromatography of *S*-diester **11**. Actually, saponification of compound **11** can be achieved, but gave tetrafluorobenzenedithiol only with low yield (25%) and insufficient purity. However, thiocarbamate **11** can be oxidatively degraded with NCS in hydrochloric acid[11] to give the bis-sulfonylchloride **12**. Since the final product **7** was difficult to purify, we took care on the purification of dichloride **12**, which was first chromatographed and then recrystallized. The yield of product **12** looks therefore low (33%), although the conversion of **11** was quantitative. Finally, hydrolysis of compound

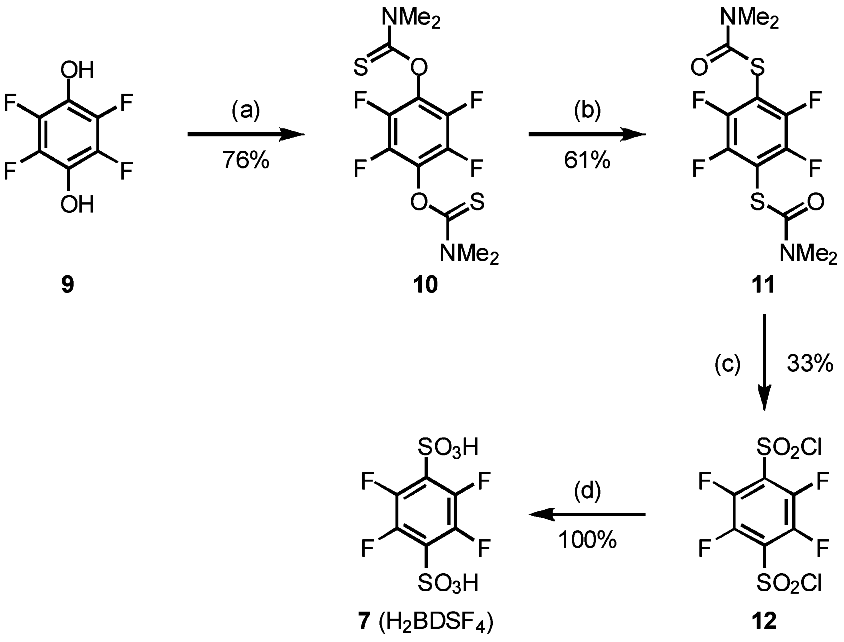

Scheme 2 Synthesis of perfluorinated disulfonic acid H_2BDSF_4 (**7**). Reagents and conditions: (a) 1. 4 eq. DABCO, 3 eq. Me_2NCSCl, DMF, 0.5 h, 35 °C; 2. 2 h, 80 °C; 3. SiO_2; (b) 1. Ph_2O, 1 h, 200 °C; 2. SiO_2; (c) 8 eq. NCS, HCl–H_2O, MeCN, 1.5 h, 10–15 °C; 2. SiO_2; 3. crystallization; (d) H_2O, 16 h, 100 °C.

12 with boiling water gave final product **7**, which was isolated after evaporation of all volatile materials as the dihydrate and in quantitative yield.

Our synthesis of the perchlorodisulfonic acid **8** started with tetrachlorobenzene **13**, the nitration of which required rather harsh conditions. Instead of handling concentrated nitric acid, we generated it *in situ* from $NaNO_3$ and boiling oleum[12] (Scheme 3). Nucleophilic displacement reactions of either one[13] or both nitro groups[14] in this product **14** with Na_2SO_3 has been reported previously to proceed smoothly. In our hands, quantitative conversion of compound **14** with Na_2SO_3 was achieved in 1,4-dioxane–H_2O at 100 °C and the disodium salt **15** was obtained in good yield, which was finally protonated in aqueous solution with a column of acidic ion exchange resin. After evaporation of all volatile materials, the free acid **8** was obtained as the trihydrate.

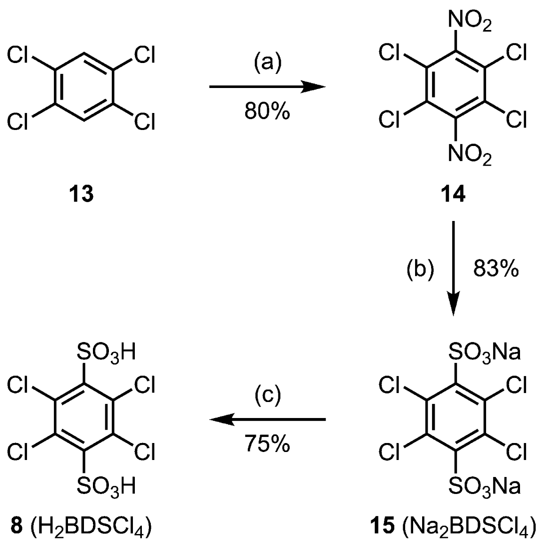

Scheme 3 Synthesis of perchlorinated disulfonic acid H_2BDSCl_4 (**8**). Reagents and conditions: (a) 6 eq. $NaNO_2$, 24 eq. H_2SO_4 with 65% SO_3, 14 h, 130 °C; (b) 5 eq. Na_2SO_3, H_2O–1,4-dioxane, 6 h, 100 °C; (c) acidic Amberlyst 15, H_2O.

Crystal structures

In the crystal structure of [Zn(BDS)(DMF)$_2$] the two crystallographically independent zinc ions, Zn1 and Zn2, are located at the Wyckoff sites 1*h* ($\frac{1}{2}$; $\frac{1}{2}$; $\frac{1}{2}$, site symmetry −1) and 1*e* ($\frac{1}{2}$; $\frac{1}{2}$; 0, site symmetry −1) of space group $P\bar{1}$. Both ions are nearly undistorted octahedrally coordinated by oxygen atoms. The oxygen atoms belong to four monodentate disulfonate groups and two DMF molecules and the distances Zn–O range from 204 to 211 pm (Zn1) and 206 to 212 pm (Zn2), respectively. The centroids of the two sulfonate groups are also located at special sites of the triclinic cell (Wyckoff positions 1*c* and 1*g*) leading to −1 symmetry for the anions in this structure. The Zn^{2+} ions are linked to infinite corrugated layers by the anions according to the formulation $^{2}_{\infty}$[Zn(BDS)$_{4/4}$(DMF)$_{2/1}$] (Fig. 1). Two oxygen atoms of each [SO_3] group are involved in the linkage, while the remaining oxygen atoms are non-coordinating. Nevertheless, the distances S–O show only slight differences with respect to each other and show typical values between 145 and 147 pm. The coordination spheres of the Zn^{2+} ions are completed by two DMF molecules which are attached *via* their oxygen atoms. The intramolecular bond distances and angles are in good agreement with previous findings for DMF complexes. The $^{2}_{\infty}$[Zn(BDS)$_{4/4}$(DMF)$_{2/1}$] layers are stacked in the [010] direction of the unit cell. The layers are held together by weak hydrogen bonds with the CH_3 groups of the solvent molecules as donors and non-coordinating oxygen atoms of the sulfonate groups as acceptors (Fig. 2). Such weak hydrogen bonds have been generally accepted since the 1980s to influence the structure of organic compounds in the solid state.[15]

The zinc salts of the tetrahalogen derivatives H_2BDSF_4 (**7**) and H_2BDSCl_4 (**8**) crystallize with four DMF molecules. The higher content of solvent molecules leads to a reduced connectivity of the anions and only one-dimensional linkage is observed. [Zn(BDSCl$_4$)(DMF)$_4$] crystallizes with triclinic symmetry and contains the Zn^{2+} ions (Wyckoff position 1*h*, $\frac{1}{2}$; $\frac{1}{2}$; $\frac{1}{2}$) with an octahedral surrounding of oxygen atoms originating from two monodentate $BDSCl_4^{2-}$ anions and four DMF molecules. The distances Zn–O are comparable to those found for [Zn(BDS)(DMF)$_2$] (207–212 pm). Also in the crystal structure

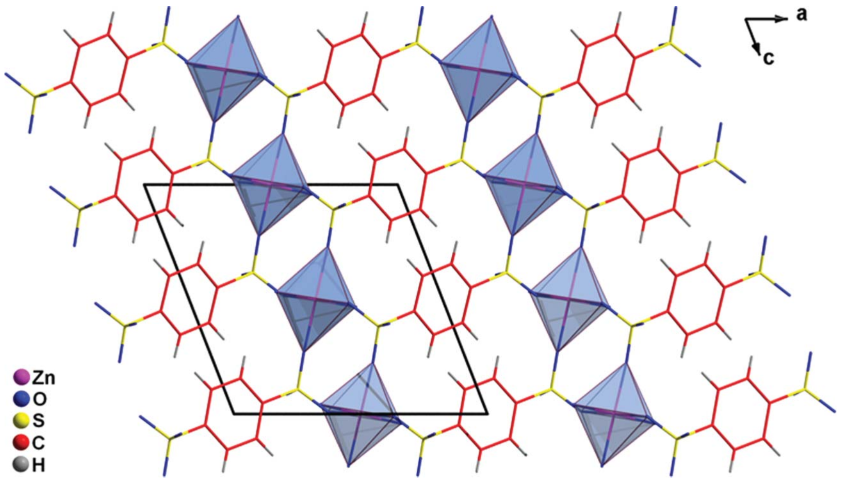

Fig. 1 Linkage of Zn^{2+} and *para*-benzenedisulfonate ions to infinite layers in the crystal structure of [Zn(BDS)(DMF)$_2$] (DMF molecules omitted for clarity).

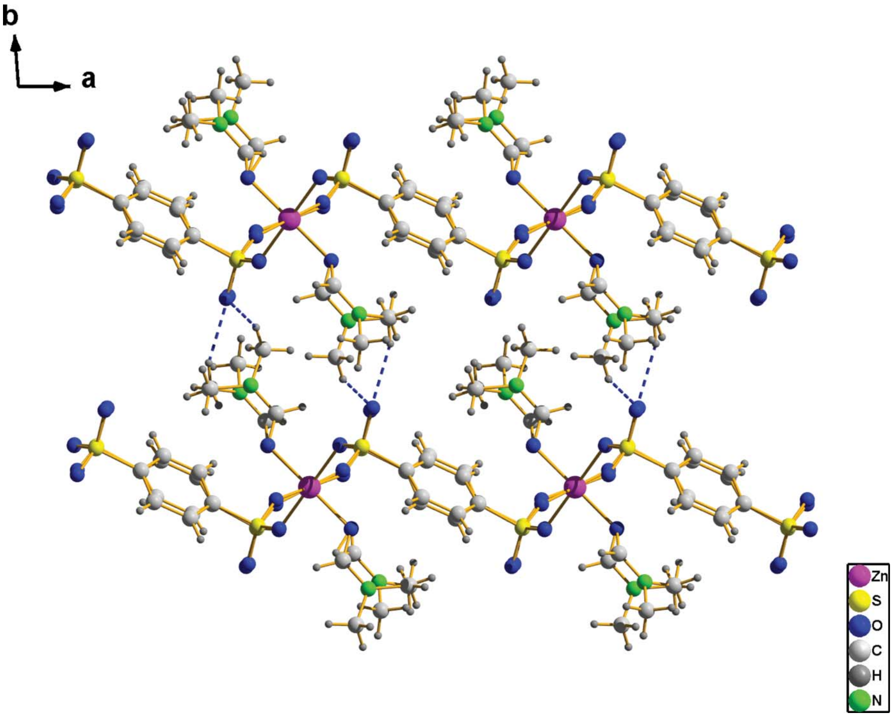

Fig. 2 Stacking of the layers shown in Fig. 1. Connection of the layers occurs by weak hydrogen bonds (dashed lines) involving DMF molecules and sulfonate groups.

of $[\mathrm{Zn(BDSCl_4)(DMF)_4}]$ the anions show inversion symmetry (centroid at Wyckoff position 1*e*, $\frac{1}{2}$; $\frac{1}{2}$; 0). While the bond distances and angles within the $[\mathrm{SO_3}]$ entity are pretty much the same as found in $[\mathrm{Zn(BDS)(DMF)_2}]$, the distance S–C is remarkably enlarged (183 *vs.* 177 pm) which might be attributed to the inductive effect of the chlorine substituents. The linkage of $\mathrm{Zn^{2+}}$ ions and $\mathrm{BDSCl_4{}^{2-}}$ anions leads to chains according to ${}^1_\infty[\mathrm{Zn(BDSCl_4)_{2/2}(DMF)_{4/1}}]$ that are oriented along the [001] direction (Fig. 3) and connected by weak hydrogen bonds (*cf.* Table 5).

The structural characteristics of $[\mathrm{Zn(BDSF_4)(DMF)_4}]$ are nearly the same as described for the chlorine derivative, although the symmetry is found to be monoclinic here (space group $P2_1/c$). The two lattices are strongly related with the *c* axis being doubled in the fluorine compound (*cf.* Table 1). The connectivity can be described accordingly as ${}^1_\infty[\mathrm{Zn(BDSF_4)_{2/2}(DMF)_{4/1}}]$ (Fig. 4). Again the $\mathrm{Zn^{2+}}$ ions and the anions are situated on positions bearing inversion symmetry (2*b* and 2*d*, respectively). For the $\mathrm{BDSF_4{}^{2-}}$ anion there is also a longer bond S–C observed (180 pm) when compared to the unsubstituted anion. The differences between the crystal structures of $[\mathrm{Zn(BDSCl_4)(DMF)_4}]$ and $[\mathrm{Zn(BDSF_4)(DMF)_4}]$ might arise from the different size of the chloro and fluoro substituents as indicated by the strongly different distances C–X (X = Cl: 172 pm, X = F: 134 pm). In order to emphasize the structural similarities of $[\mathrm{Zn(BDSF_4)(DMF)_4}]$ and $[\mathrm{Zn(BDSCl_4)(DMF)_4}]$ the latter was described in an unconventional setting of space group $P\bar{1}$ in Table 1. Table 3 compares the imported structural parameters of the zinc sulfonates.

In the triclinic crystal structure of $[\mathrm{Cu(H_2O)_6}](\mathrm{BDSF_4})$ the $\mathrm{Cu^{2+}}$ ions are located at the Wyckoff position 1*e* ($\frac{1}{2}$; $\frac{1}{2}$; 0) and coordinated by three crystallographically different water molecules (Fig. 5). The distances Cu–O are 195, 198, and 239 pm, indicating the typical Jahn–Teller distortion. The centroid of the completely planar $\mathrm{BDSF_4{}^{2-}}$ dianion is also located at a position with inversion symmetry (1*f*, $\frac{1}{2}$; 0; $\frac{1}{2}$). The observed distances within the anion are comparable to those described for $[\mathrm{Zn(BDSF_4)(DMF)_4}]$ (*cf.* Table 4). Between the water molecules of the complex cations and the oxygen atoms of the anions medium strong hydrogen bonds can be assumed with respect to the observed donor–acceptor distances. Also some fluorine atoms may contribute to the hydrogen bonds (Table 5).[15]

In contrast to the findings for $[\mathrm{Cu(H_2O)_6}](\mathrm{BDSF_4})$, the orthorhombic crystal structure of $[\mathrm{Cu(BDSCl_4)(H_2O)_4}]$ exhibits a one-dimensional structure with the $\mathrm{Cu^{2+}}$ ions linked by $\mathrm{BDSCl_4{}^{2-}}$ ligands according to ${}^1_\infty[\mathrm{Cu(BDSCl_4)_{2/2}(H_2O)_{4/1}}]$ (Fig. 6). The coordination sphere of the copper ions, which are located on the special sites 4*a* (0; 0; 0, site symmetry −1), is completed by four water molecules and the coordination polyhedron is again Jahn–Teller distorted. The water molecules show distances of 194 and 196 pm, respectively. The distances Cu–O to the oxygen atoms of the sulfonate ligands are 244 pm. The two coordinating oxgen atoms are in relative *syn*-conformation at the benzene ring. The chains ${}^1_\infty[\mathrm{Cu(BDSCl_4)_{2/2}(H_2O)_{4/1}}]$ are zigzag shaped and running along the [001] direction of the unit cell. Connection between the chains is achieved by hydrogen bonds which involve the water molecules as donors and both non-coordinating oxygen atoms of the sulfonate groups and even chlorine atoms of the substituted benzene ring as acceptors. The latter type of hydrogen bonds has been described in some cases and the observed donor–acceptor distances hint at only weak interactions (Table 5).[16] The orientation of the infinite chains with respect to each other leads to a stacking of hydrophobic and hydrophilic domains along the [010] direction (*cf.* Fig. 6).

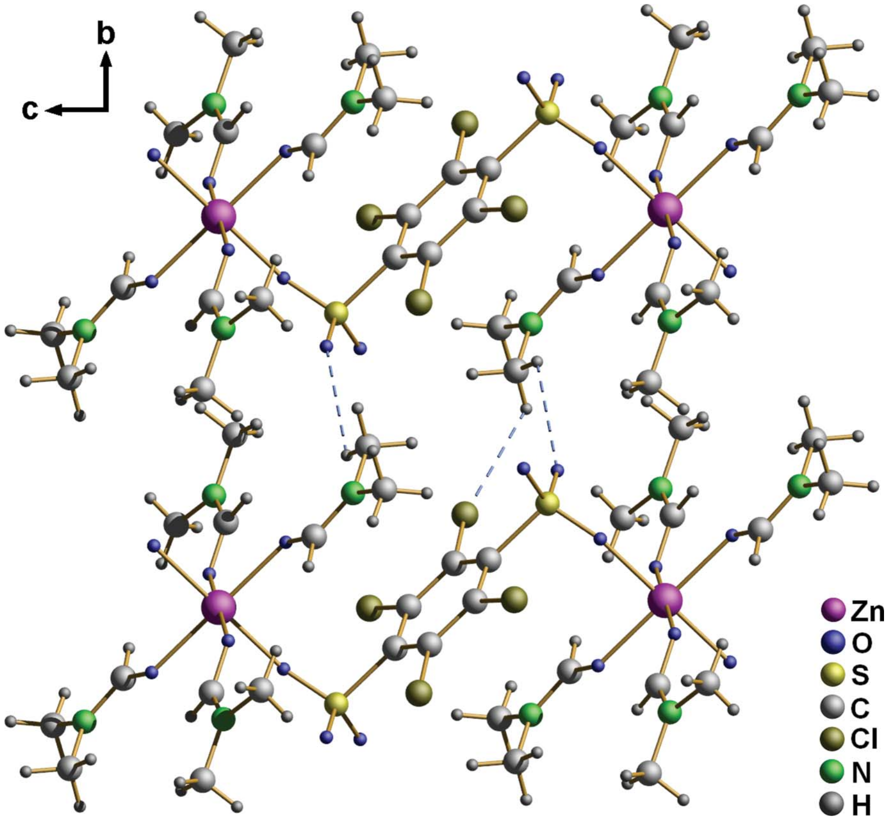

Fig. 3 Crystal structure $[Zn(BDSCl_4)(DMF)_4]$. The $BDSCl_4^{2-}$ anions connect the Zn^{2+} ions to chains that are held together by hydrogen bonds.

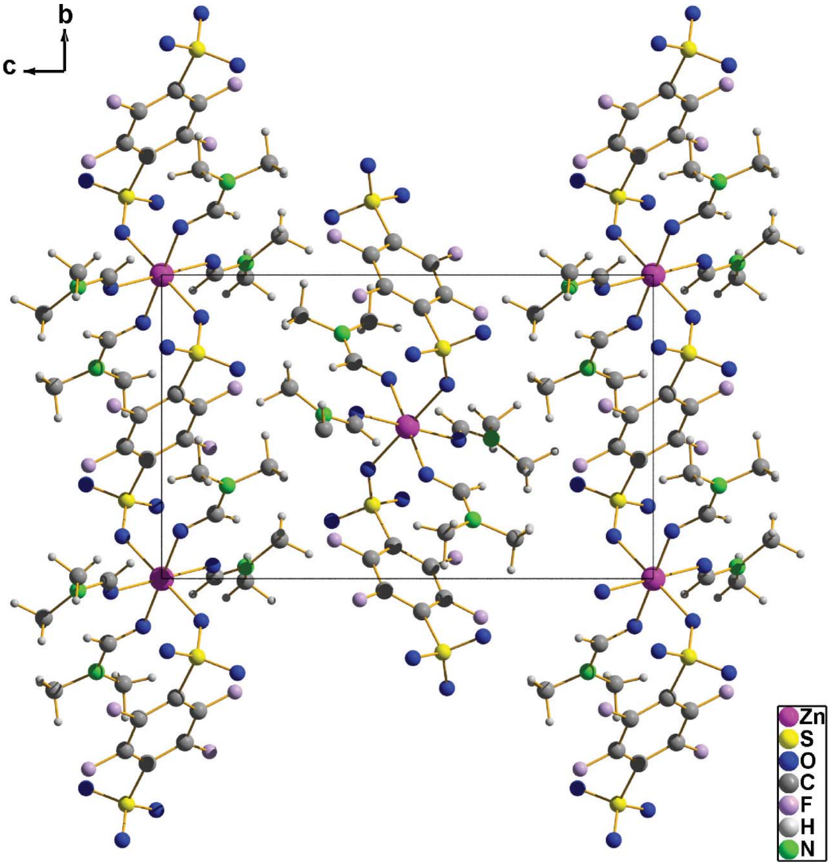

Fig. 4 Arrangement of the chains $^{1}_{\infty}[Zn(BDSF_4)_{2/2}(DMF)_{4/1}]$ in the crystal structure of $[Zn(BDSF_4)(DMF)_4]$.

Table 1 Crystallographic data of [Zn(BDS)(DMF)$_2$], [Zn(BDSCl$_4$)(DMF)$_4$], and [Zn(BDSF$_4$)(DMF)$_4$] and their determination

	[Zn(BDS)(DMF)$_2$]	[Zn(BDSCl$_4$)(DMF)$_4$]	[Zn(BDSF$_4$)(DMF)$_4$]
chemical formula	$C_{12}H_{18}N_2O_8S_2Zn$	$C_{18}H_{28}Cl_4N_4O_{10}S_2Zn$	$C_{18}H_{28}F_4N_4O_{10}S_2Zn$
chemical formula weight	447.77	731.73	665.93
lattice parameters	$a = 976.62(4)$ pm	$a = 905.2(1)$ pm	$a = 889.01(3)$ pm
	$b = 986.85(4)$ pm	$b = 989.6(1)$ pm	$b = 968.91(3)$ pm
	$c = 1014.40(4)$ pm	$c = 831.5(1)$ pm	$c = 1633.07(5)$ pm
	$\alpha = 69.106°(2)$	$\alpha = 91.41°(2)$	
	$\beta = 68.746°(2)$	$\beta = 106.72°(2)$	$\beta = 106.524°(2)$
	$\gamma = 86.295°(2)$	$\gamma = 90.44°(2)$	
density (calculated, g cm^{-3})	1.752	1.704	1.731
cell volume	848.89(6) Å^3	713.0(2) Å^3	1348.58(7) Å^3
no. of formula units	2	1	2
cryst. syst.	triclinic	triclinic	monoclinic
space group	$P\bar{1}$ (No. 2)	$P\bar{1}$ (No. 2)	$P2_1/c$ (No. 14)
measuring device	Bruker APEX II	Stoe IPDS I	Bruker APEX II
radiation	Mo-Kα (graphite monochromatized, $\lambda = 71.07$ pm)	Mo-Kα (graphite monochromatized, $\lambda = 71.07$ pm)	Mo-Kα (graphite monochromatized, $\lambda = 71.07$ pm)
temperature	153 K	153 K	153 K
θ range	$4.62° < 2\theta < 70°$	$5.86° < 2\theta < 56.56°$	$4.94° < 2\theta < 70.38°$
rotation angle, φ-increment	—	$0.0° < \varphi < 320°$; 2.0°	—
index range	$-15 \leq h \leq 14$	$-12 \leq h \leq 12$	$-14 \leq h \leq 14$
	$-15 \leq k \leq 15$	$-13 \leq k \leq 13$	$-8 \leq k \leq 15$
	$-16 \leq l \leq 16$	$-11 \leq l \leq 11$	$-24 \leq l \leq 26$
no. of exposures	—	160	—
exposure time	—	1.5 min	—
detector distance	—	60 mm	—
absorption correction	numerical	numerical	numerical
μ	17.37 cm^{-1}	14.40 cm^{-1}	20.17 cm^{-1}
measured reflections	30921	11246	25846
unique reflections	7458	3226	5836
with $I_0 > 2\sigma(I_0)$	4895	2699	3269
R_{int}; R_σ	0.0389; 0.0351	0.0428; 0.0329	0.0616; 0.0984
structure determination	SHELXS97 and SHELXL97	SHELXS97 and SHELXL97	SHELXS97 and SHELXL97
scattering factors	Intern. Tables, Vol. C	Intern. Tables, Vol. C	Intern. Tables, Vol. C
GOF	0.873	0.995	0.880
R_1; wR_2 ($I_0 > 2\sigma(I_0)$)	0.0233; 0.0582	0.0252; 0.0628	0.0348; 0.0679
R_1; wR_2 (all data)	0.0423; 0.0627	0.0317; 0.0647	0.0884; 0.0948
max./min. electron density	0.635/−0.474 e Å^{-3}	0.460/−0.462 e Å^{-3}	0.499/−0.803 e Å^{-3}
CCDC number	763637	763638	763639

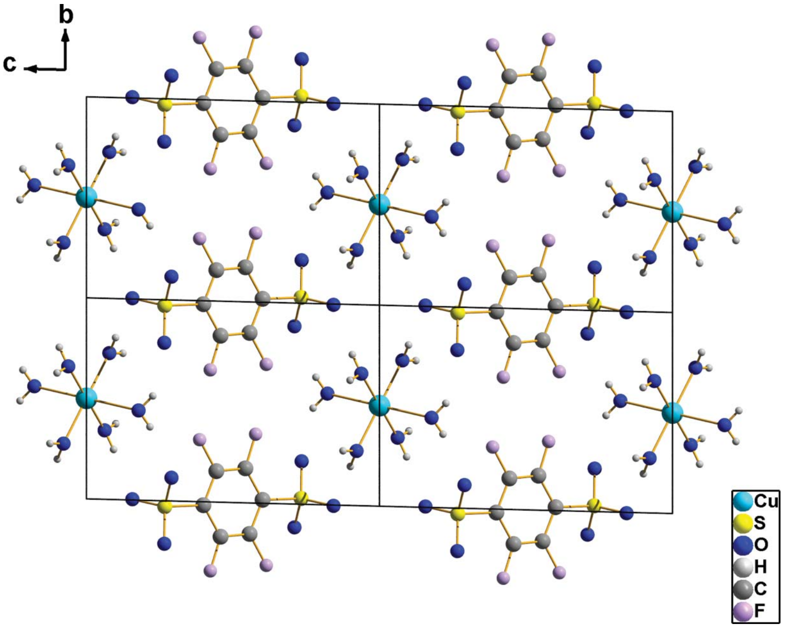

Fig. 5 Crystal structure of [Cu(H$_2$O)$_6$](BDSF$_4$) with complex [Cu(H$_2$O)$_6$]$^{2+}$ cations and non-coordinating sulfonate anions.

Table 2 Crystallographic data of $[Cu(H_2O)_6](BDSF_4)$, $[Cu(BDSCl_4)(H_2O)_4]$, and $Na_2BDSCl_4{\cdot}2H_2O$ and their determination

	$[Cu(H_2O)_6](BDSF_4)$	$[Cu(BDSCl_4)(H_2O)_4]$	$Na_2BDSCl_4{\cdot}2H_2O$
chemical formula	$C_6H_{12}CuF_4O_{12}S_2$	$C_6H_8Cl_4CuO_{10}S_2$	$C_6H_4Cl_4Na_2O_8S_2$
chemical formula weight	479.82	509.58	455.68
lattice parameters	$a = 510.45(2)$ pm	$a = 721.27(2)$ pm	$a = 1156.7(2)$ pm
	$b = 744.68(3)$ pm	$b = 2147.81(6)$ pm	$b = 558.47(5)$ pm
	$c = 1077.77(4)$ pm	$c = 979.42(3)$ pm	$c = 1072.3(2)$ pm
	$\alpha = 85.627(2)°$		
	$\beta = 77.449(2)°$		$\beta = 91.49(2)°$
	$\gamma = 76.015(2)°$		
density (calculated) [g cm^{-3}]	2.054	2.231	2.187
cell volume	387.92(3) Å^3	1517.27(8) Å^3	692.5(2) Å^3
no. of formula units	1	4	4
cryst. syst.	triclinic	orthorhombic	monoclinic
space group	$P\bar{1}$ (No. 2)	*Pnma* (No. 62)	$P2_1/c$
measuring device	Bruker APEX II	Bruker APEX II	STOE IPDS I
radiation	Mo-Kα (graphite monochromatized, $\lambda = 71.07$ pm)	Mo-Kα (graphite monochromatized, $\lambda = 71.07$ pm)	Mo-Kα (graphite monochromatized, $\lambda = 71.07$ pm)
temperature	153 K	153 K	153 K
θ range	$5.64° < 2\theta < 80.60°$	$7.02° < 2\theta < 70.14°$	$7.04° < 2\theta < 56.56°$
rotation angle, φ-increment	—	—	$0.0° < \varphi < 300°$; 2.0
index range	$-9 \le l \le 9$	$-9 \le l \le 11$	$-15 \le l \le 15$
	$-12 \le l \le 13$	$-34 \le l \le 34$	$-6 \le l \le 6$
	$-19 \le l \le 19$	$-15 \le l \le 15$	$-14 \le l \le 14$
absorption correction	numerical	numerical	numerical
μ	17.83 cm^{-1}	24.66 cm^{-1}	12.56 cm^{-1}
measured reflections	20526	26926	9049
unique reflections	4896	3403	1588
with $I_0 > 2\sigma(I_0)$	4069	3046	1389
R_{int}; R_σ	0.0362; 0.0276	0.0244; 0.0140	0.0234
structure determination	SHELXS97 and SHELXL97	SHELXS97 and SHELXL97	SHELXS97 and SHELXL97
scattering factors	Intern. Tables, Vol. C	Intern. Tables, Vol. C	Intern. Tables, Vol. C
GOF	1.059	1.032	1.018
R_1; wR_2 ($I_0 > 2\sigma(I_0)$)	0.0265; 0.0746	0.0266; 0.0707	0.0195/0.0511
R_1; wR_2 (all data)	0.0336; 0.0770	0.0308; 0.0736	0.0234/0.0523
max./min. electron density	1.166/−0.815 e Å^{-3}	2.004/−1.370 e Å^{-3}	0.418/−0.257 e Å^{-3}
CCDC number	777578	776934	776935

The most remarkable structural feature of $[Cu(BDSCl_4)(H_2O)_4]$ is however the non-planarity of the benzene ring, which adopts a boat conformation (Fig. 7a). Neither the chlorine atoms nor the carbon atoms in the 1- and 4-position of the ring (as well as the sulfur atoms of the sulfonate groups) are within the plane defined by the four remaining carbon atoms of the benzene ring. The deviation from the plane is 8.5° (distance from the plane: 29.7 pm) for the carbon atoms, and 9° (23.7 and 24.4 pm) the chlorine atoms. Small distortion from planarity is a very seldom seen effect for benzene derivatives.[17] However, it is the general case for benzene rings with multiple donor and acceptor substituents.[18]

In order to elucidate, whether this is an intrinsic effect of the $BDSCl_4^{2-}$ anion, we investigated single crystals of the disodium salt $Na_2BDSCl_4{\cdot}2H_2O$ (Table 2). In the monoclinic structure the anions are located of the Wyckoff position 2*c* (0; 0; $\frac{1}{2}$) and stacked along the [001] axis of the unit cell. Charge balance is achieved by Na^+ ions that are five-fold coordinated by three oxygen atoms of sulfonate groups and two H_2O molecules (Fig. 8). Interestingly in this compound the benzene ring is completely planar (Fig. 7b), so that a steric effect within the aromatic ring can be ruled out as the mechanism for non-planarity of the anion in $[Cu(BDSCl_4)(OH_2)_4]$. The main difference between the anions in the two crystal structures is the orientation of the sulfo groups with respect to the benzene ring. In the copper compound they are in a relative *syn* conformation, *i.e.* the sulfonate oxygen atoms are arranged ecliptic when viewed along a virtual connecting line between both sulfur atoms, while their arrangement is staggered in the case of the sodium compound (Fig. 9). A deeper insight into the non-planarity phenomenon of the $BDSCl_4^{2-}$ anion in the copper compound was achieved by *ab intio* calculations reported in the next subsection.

Computational results

Calculations were performed for H_2BDSF_4, H_2BDSCl_4, and the anion $BDSCl_4^{2-}$. Furthermore, the tetrabromo and tetraiodo derivatives H_2BDSBr_4 and H_2BDSI_4 were included for comparison. First of all, a full geometry optimization of H_2BDSF_4 did not reveal any significant distortion of the planar ring geometry. By starting from the experimental value of the out-of-plane angle for H_2BDSCl_4, the final H_2BDSF_4 geometry resulted in a deviation of the plane of only 0.8°. This is in agreement with experiment and in contrast to the corresponding calculations of H_2BDSCl_4. Here, a pronounced boat geometry is found for the *syn* conformation where the OH-moieties of sulfonate groups are located on the same side of the aromatic ring. Starting from a planar initial geometry, the out-of-plane angle was found to be 6.7°. However, this structure was found to be a local minimum only. In the *anti* conformation the OH-moieties of the sulfonate groups are located on different sides of the aromatic ring which results in a slightly more stable conformation, although the energetic difference of 0.03 eV is very small. In this conformation the out of plane angle

Table 3 Selected distances (pm) and angles (deg.) for the zinc compounds

	$[Zn(BDS)(DMF)_2]$				$[Zn(BDSCl_4)(DMF)_4]$				$[Zn(BDSF_4)(DMF)_4]$			
$[ZnO_6]$	Zn1	-O1	204.06(7)		Zn1	-O1	205.7(1)		Zn1	-O1	207.2(1)	
		-O11	211.87(7)			-O2	211.3(1)			-O2	209.2(1)	
		-O21	211.46(7)			-O11	211.2(1)			-O11	211.5(1)	
	Zn2	-O2	206.39(7)									
		-O12	211.92(7)									
		-O22	208.49(7)									
	O1-	Zn1	-O11	86.05(3)	O1-	Zn1	-O2	89.77(5)	O1-	Zn1	-O2	89.79(5)
	O1-	Zn1	-O21	87.71(3)	O1-	Zn1	-O11	89.04(5)	O1-	Zn1	-O11	86.95(5)
	O21-	Zn1	-O11	89.37(3)	O2-	Zn1	-O11	88.31(5)	O2-	Zn1	-O11	89.54(5)
	O2-	Zn2	-O12	87.69(3)								
	O2-	Zn2	-O22	85.15(3)								
	O22-	Zn2	-O12	89.01(3)								
$[SO_3]$	S1	-O11	145.41(8)		S1	-O11	146.3(1)		S1	-O11	145.9(1)	
		-O12	147.07(7)			-O12	143.8(1)			-O12	144.3(1)	
		-O13	144.64(8)			-O13	144.4(1)			-O13	143.5(1)	
		-C11	177.1(1)			-C11	182.8(2)			-C11	180.5(2)	
	S2	-O21	146.56(7)									
		-O22	145.84(8)									
		-O23	144.82(8)									
		-C21	177.1(1)									
	O11-	S1	-O12	112.53(5)	O11-	S1	-O12	112.49(8)	O11-	S1	-O12	111.68(8)
	O11-	S1	-O13	114.20(5)	O11-	S1	-O13	111.89(7)	O11-	S1	-O13	114.14(8)
	O12-	S1	-O13	111.38(5)	O12-	S1	-O13	115.12(8)	O12-	S1	-O13	115.19(9)
	O11-	S1	-C11	105.53(5)	O11-	S1	-C11	104.44(7)	O11-	S1	-C11	103.98(8)
	O12-	S1	-C11	106.43(4)	O12-	S1	-C11	108.48(7)	O12-	S1	-C11	104.15(8)
	O13-	S1	-C11	106.05(5)	O13-	S1	-C11	103.36(7)	O13-	S1	-C11	106.35(8)
	O21-	S2	-O22	112.43(5)								
	O21-	S2	-O23	111.96(5)								
	O22-	S2	-O23	114.00(5)								
	O21-	S2	-C21	106.56(4)								
	O22-	S2	-C21	104.62(5)								
	O23-	S2	-C21	106.51(5)								
	O11-	S1	-O12	112.53(5)								

Table 4 Selected distances (pm) and angles (deg.) for the copper compounds

	$[Cu(H_2O)_6](BDSF_4)$				$[Cu(BDSCl_4)(H_2O)_4]$			
$[CuO_6]$	Cu1	-O1		197.68(8)	Cu1	-O1		194.0(1)
		-O2		237.86(9)		-O2		195.8(1)
		-O3		194.58(8)		-O11		244.8(1)
	O1-	Cu1	-O2	87.01(3)	O1-	Cu1	-O2	88.30(4)
	O1-	Cu1	-O3	86.48(3)	O1-	Cu1	-O11	88.84(4)
	O2-	Cu1	-O3	86.41(3)	O2-	Cu1	-O11	88.50(4)
$[SO_3]$	S1	-O11		144.00(8)	S1	-O11		144.3(1)
		-O12		146.20(8)		-O12		146.3(1)
		-O13		145.40(8)		-O13		146.2(1)
		-C11		178.7(1)		-C11		180.9(2)
	O11-	S1	-O12	113.31(5)	O11-	S1	-O12	115.04(6)
	O11-	S1	-O13	113.52(5)	O11-	S1	-O13	111.91(6)
	O12-	S1	-O13	112.50(5)	O12-	S1	-O13	111.43(6)
	O11-	S1	-C11	106.12(5)	O11-	S1	-C11	106.34(6)
	O12-	S1	-C11	104.15(4)	O12-	S1	-C11	104.95(6)
	O13-	S1	-C11	106.30(5)	O13-	S1	-C11	106.40(6)

was found to be only 0.2°. These results are in good agreement with experiment since the boat conformation of the aromatic ring is found only for the Cu(II)-salt, in which coordination also occurs on the same side of the ring. In the sodium salt, $BDSCl_4^{2-}$ can be regarded as a "free" dianionic species, in which *syn* coordination does not occur, resulting in a planar aromatic system. This is corroborated by our geometry optimization of free $BDSCl_4^{2-}$ in which a planar conformation is obtained.

As far as the origin of a local minimum of *syn* H_2BDSCl_4 is concerned, steric effects play a significant role. We substituted –Cl by –Br and –I and found even larger out-of-plane angles of 12.6° and 17.5°, respectively. A steric mechanism seems further conclusive since the substitution of both sulfonate groups by *tert*-butyl moieties rules out electronic effects and results in an out-of-plane angle of 18.6°.

Thermal analysis

The desolvation of $[Zn(BDS)(DMF)_2]$ takes place in the temperature range between 55 and 210 °C and three steps can be identified in the DTG curve (Fig. 10). The desolvation is complete according to the observed mass loss of 34.7% (calcd. 32.6%). The solvent-free compound [Zn(BDS)] is thermally stable up to nearly 600 °C. At this temperature a hitherto unknown intermediate is formed that decomposes further leading to ZnS in the wurtzite type of

Table 5 Selected hydrogen bonds

D–H	d(D–H)/pm	d(H...A)/pm	∠DHA/°	d(D...A)/pm	A
[Zn(BDSCl$_4$)(DMF)$_4$]					
C2–H22	90(2)	261(3)	148(1)	341.4(2)	O12
C3–H32	95(2)	285(3)	106(1)	343.3(2)	Cl1
C5–H53	99(2)	244(2)	168(2)	342.0(2)	O13
C5–H52	91(2)	297(3)	159(2)	384.2(3)	Cl1
[Zn(BDSF$_4$)(DMF)$_4$]					
C3–H33	103(2)	260(2)	130(2)	331.1(2)	O12
C3–H31	96(2)	270(2)	152(2)	358.4(3)	F1
C5–H52	96(2)	248(2)	165(1)	341.2(2)	O12
C5–H51	96(2)	267(3)	115(2)	320.0(2)	F2
[Cu(H$_2$O)$_6$](BDSF$_4$)					
O1-H11	78(2)	196(2)	179(2)	274.1(2)	O12
O1-H12	76(2)	207(3)	167(2)	282.2(3)	O13
O2-H21	73(2)	201(2)	168(1)	273.4(2)	O11
O2-H22	76(2)	212(2)	145(2)	277.0(2)	O13
O2-H22	76(2)	245(2)	143(1)	309.1(3)	F1
O3-H32	79(2)	195(2)	176(2)	272.8(2)	O12
O3-H31	79(2)	189(2)	173(2)	266.9(2)	O2
[Cu(BDSCl$_4$)(H$_2$O)$_4$]					
O1–H11	79(2)	192(2)	171(2)	270.0(2)	O13
O1–H11	79(2)	296(3)	118(1)	340.2(3)	Cl2
O1–H12	76(2)	193(2)	174(2)	268.6(2)	O13
O2–H21	78(2)	198(2)	174(2)	275.2(2)	O12
O2–H22	76(2)	203(2)	177(2)	278.8(3)	O12

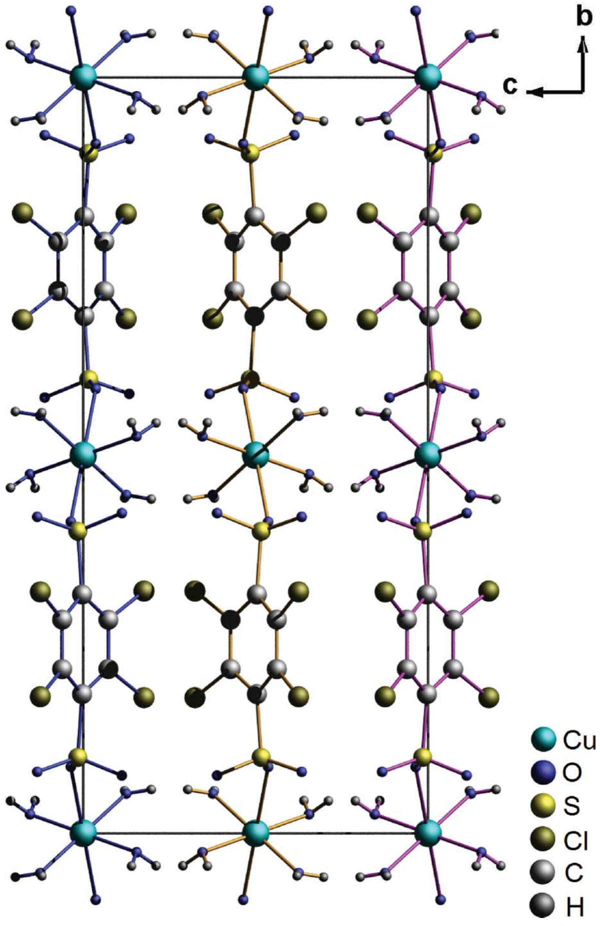

Fig. 6 Chain structure of [Cu(BDSCl$_4$)(H$_2$O)$_4$]. The coordination sphere of the copper ions is completed by water molecules.

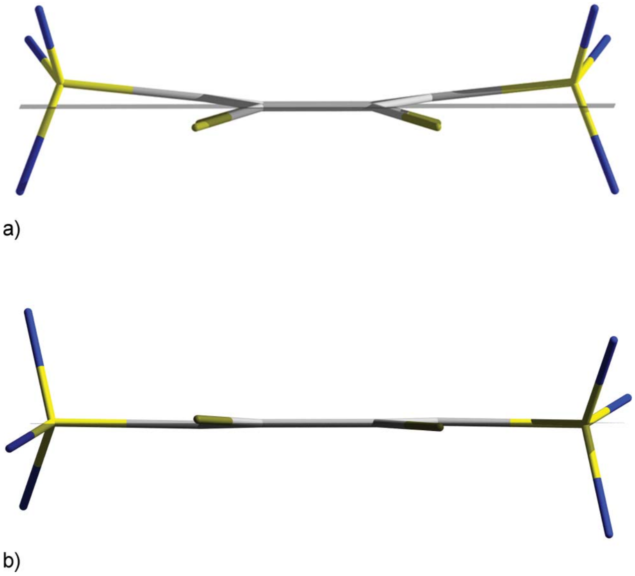

Fig. 7 The p-BDSCl$_4$ anion in [Cu(BDSCl$_4$)(H$_2$O)$_4$] (a) and Na$_2$BDSCl$_4$·2H$_2$O (b). In the copper compound a remarkable deviation of the benzene ring towards a boat conformation is observed while the sodium compound exhibits the planar anion.

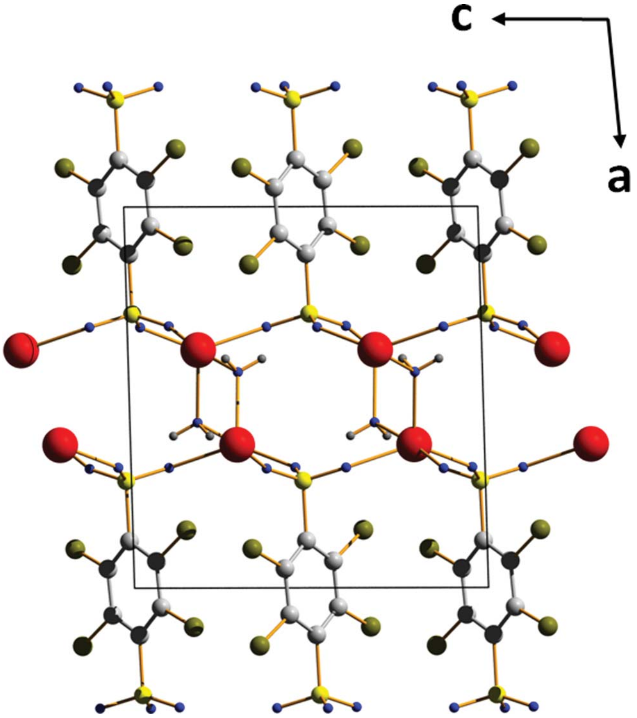

Fig. 8 Crystal structure of Na$_2$BDSCl$_4$·2H$_2$O. The structure shows a close relation to the structure of [Cu(BDSCl$_4$)(H$_2$O)$_4$] (*cf.* Fig. 6).

structure according to the observed XRD powder pattern. The thermal decomposition of [Zn(BDSF$_4$)(DMF)$_4$] starts also with the release of the solvent molecules. Two steps can be clearly identified (Fig. 10) and a small shoulder for one of the peaks indicated that there might be a third step. Desolvation is completed at 220 °C (mass loss: 40.3%, calcd. 41.6%) and the decomposition

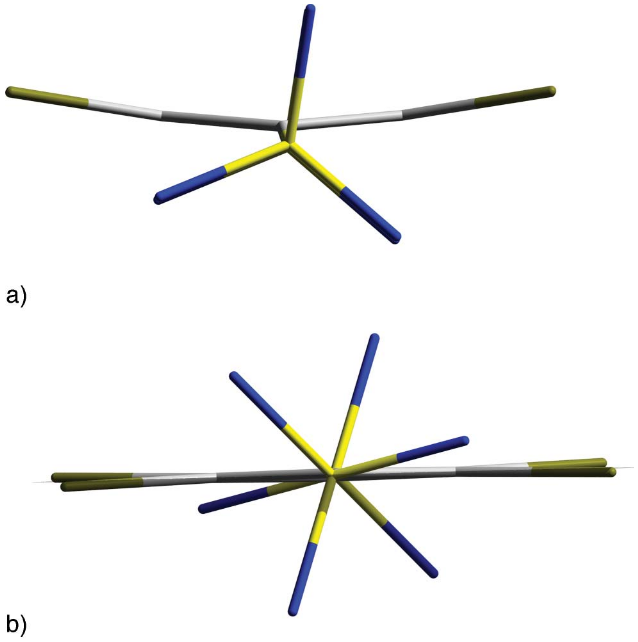

Fig. 9 Comparison of the *p*-$BDSCl_4$ conformation in $[Cu(BDSCl_4)(H_2O)_4]$ (a) and $Na_2BDSCl_4{\cdot}2H_2O$ (b). The anions are shown along a virtual line connecting the sulfur atoms of the $[SO_3]$ moieties.

of the remaining $[Zn(BDSF_4)]$ occurs in the temperature range between 470 and 560 °C. After that temperature a continuing weight loss can be seen in the TG curve. According to XRD measurements the residue is hexagonal zinc oxide. For the chlorine derivative $[Zn(BDSCl_4)(DMF)_4]$ the loss of solvent molecules is completed at 190 °C (Fig. 10). The desolvated compound decomposes in a two step process starting at 330 °C leading to an unknown intermediate that was degraded further at about 750 °C, again yielding ZnO.

The thermal decomposition of the copper disulfonates $[Cu(H_2O)_6](BDSF_4)$ and $[Cu(BDSCl_4)(H_2O)_4]$ starts with dehydration of the compounds (Fig. 11). For the hexahydrate three steps can be identified and the dehydration ends at 245 °C (mass loss: 22.8% obsd., 22.6% calcd.). The anhydrous compound decomposes between 300 and 460 °C with CuO as the residue as identified by XRD. The tetrahydrate of the chlorine derivative loses the water molecules in two steps and the dehydration is complete at 280 °C (mass loss: 14.0% obsd., 14.1% calcd.). The anhydrous compound $[Cu(BDSCl_4)(H_2O)_4]$ decomposes to an unknown intermediate at 405 °C. The latter is finally transformed to elemental copper in a broad temperature range between 500 and 650 °C. As can be seen from the XRD pattern of $[Cu(BDSCl_4)(H_2O)_4]$ after dehydration at 300 °C the anhydrous compound still shows a good crystallinity (Fig. 12).

Discussion and conclusion

The enhancement of both structural diversity and thermal stability of metal–organic-frameworks requires new types of linker molecules. The majority of linkers that are actually used for building MOFs are carboxylates. They are easily accessible but their thermal stability is limited. Switching to sulfonates promises increased thermal stability but on the other hand the synthesis of polysulfonic acids is tedious. Simple sulfonation by electrophilic substitution of benzene is not a good option because the sulfonate group is deactivating and *meta*-directing. These preparative difficulties are the main reason that reports on polysulfonates are very limited although it has been mentioned several times that they seem worthwhile to be investigated. Thus, the key step of our research program was to develop synthetic strategies that allow the production of multigram amounts of polysulfonic acids using cheap chemicals. A simple and effective route to *para*-benzene disulfonic acid H_2BDS (**4**) as analogue of terephthalic acid (**1**) has been reported previously by us. In the present paper we present convenient routes to the tetrahalogen derivatives H_2BDSF_4 (**7**) and H_2BDSCl_4 (**8**) from readily available starting materials. The tetrafluoro-congener **7** is prepared in

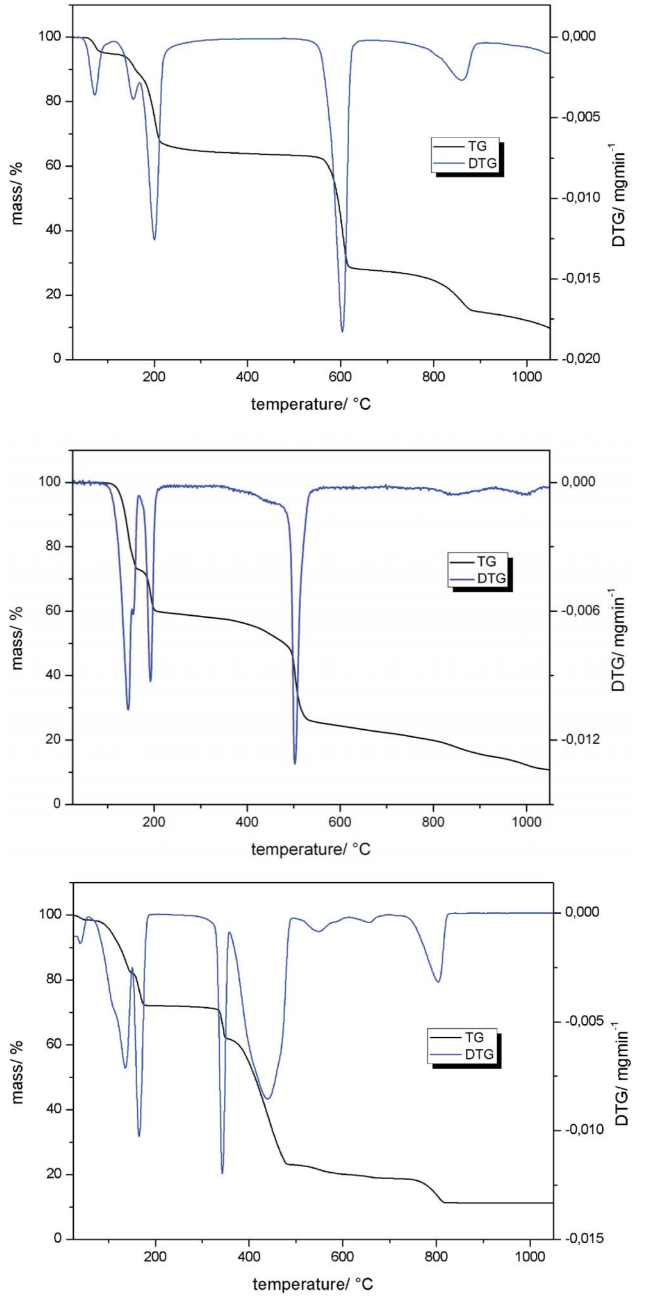

Fig. 10 TG/DTG diagrams for $[Zn(BDS)(DMF)_2]$ (top), $[Zn(BDSF_4)(DMF)_4]$ (middle) $[Zn(BDSCl_4)(DMF)_4]$ (bottom).

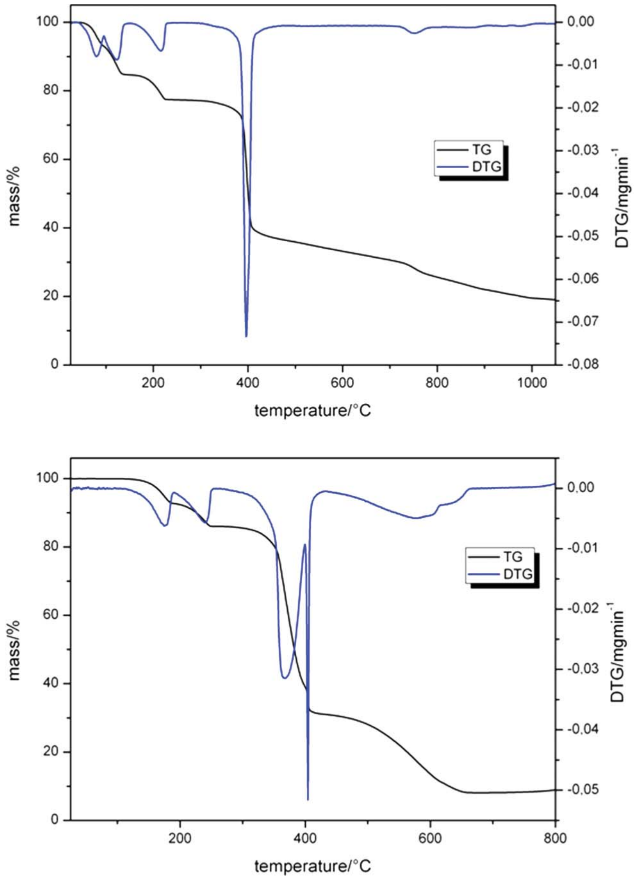

Fig. 11 TG/DTG diagrams for $[Cu(H_2O)_6](BDSF_4)$ (top) and $[Cu(BDSCl_4)(H_2O)_4]$ (bottom).

four steps from tetrafluorohydroquinone (**9**) with 15% overall yield. The three-step synthesis of H_2BDSCl_4 (**8**) starts from tetrachlorobenzene (50% overall yield).

Table 6 Characteristics of the compounds investigated

Compound	Dim. of linkage	Temp. range of desolvation/°C	Temp. range of decomposition/°C
$[Cu(H_2O)_6](BDSF_4)$	0	40–245	300–460
$[Cu(BDSCl_4)(H_2O)_4]$	1	95–280	360–440
$[Zn(BDSF_4)(DMF)_4]$	1	100–220	470–560
$[Zn(BDSCl_4)(DMF)_4]$	1	35–190	330–470
$[Zn(BDS)(DMF)_2]$	2	55–210	552–625

The second step of our research program was to attempt the building of MOFs based on the new polysulfonic acids and to explore the properties of the compounds obtained (Table 6). The zinc compounds were obtained from DMF solutions. In all of the compounds solvent molecules act as ligands for the Zn^{2+} ions, so that no three-dimensional linkage occurs. The same is true for the copper sulfonates where strong coordination of the solvent water molecules is observed. This is a typical finding for sulfonates of harder cations.[19] Even if other preparative conditions may lead to solvent-free compounds, the simplest way to these phases is thermal desolvation. With respect to our thermoanalytical investigations the presented sulfonates show a large temperature range between complete desolvation and decomposition of the ligands. The thermal stability is remarkably high compared to the respective carboxylates. Typical temperatures for the decomposition of copper carboxylates are reported to lie at about 250 °C, the respective zinc compounds decompose at about 375 °C.[20] Fluorine and chlorine derivatives of these carboxylates decompose at even lower temperature.[6a,21] As has been demonstrated for $[Cu(BDSCl_4)(H_2O)_4]$, the dehydration at 300 °C leads to a crystalline anhydrous compound (Fig. 12). It can be assumed that this compound shows a three-dimensional network, but only a structure determination can reveal the connectivity and the porosity of the compound. These structure elucidations have also to be done for the other desolvated phases to prove the thermoanalytical results. Moreover it would be of utmost interest to investigate the conformation of the $BDSCl_4^{2-}$ anion in the

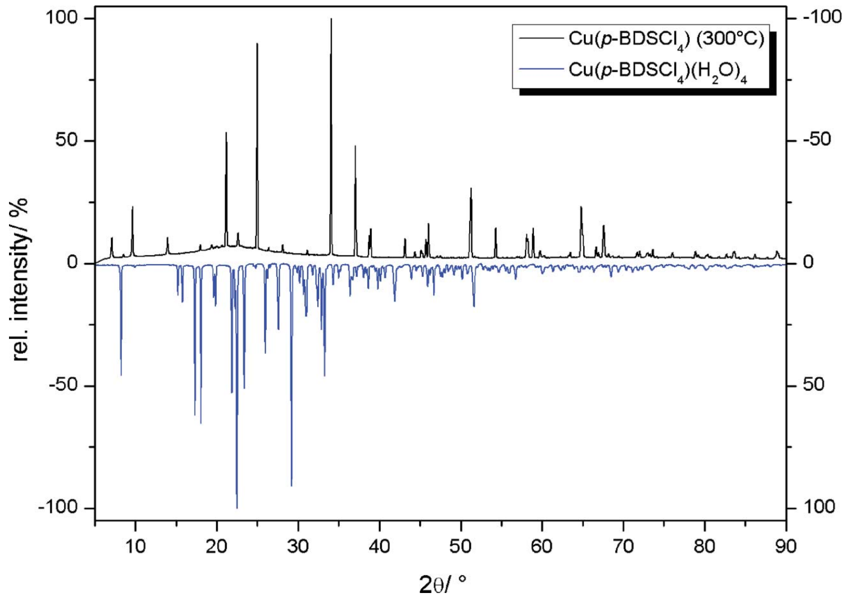

Fig. 12 XRD patterns for $[Cu(BDSCl_4)(H_2O)_4]$ and the dehydrated phase $[Cu(BDSCl_4)]$.

anhydrous phase. We assume that the deviation from planarity is correlated to the arrangement of the [SO_3] groups with respect to each other and thus occurs as a result of steric hindrance. This hypothesis is further corroborated by the larger extent of distortion in cases where larger moieties such as bromine, iodine or *tert*-butyl were used as substituents.

In conclusion we are convinced that we have provided facile routes to polysulfonic acids and that their availability will have a remarkable impact in MOF chemistry.

Experimental Section

General methods. Preparative column chromatography was carried out using Merck SiO_2 (0.035–0.070 mm, type 60 A) with hexane, *tert*-butylmethylether (MTBE) and CH_2Cl_2 as eluents. TLC was performed on Merck SiO_2 F_{254} plates on aluminium sheets. ^{1}H-, ^{13}C- and ^{19}F-NMR spectra were recorded on a Bruker Avance DRX 500 spectrometer. Multiplicities were determined with DEPT experiments. IR spectra were recorded on a Bruker Tensor 27 spectrometer equipped with a "GoldenGate" diamond-ATR unit. EI-MS and HRMS spectra were obtained with a Finnigan MAT 95 spectrometer, ESI-MS (HRMS) spectra with a Waters Q-TOF Premier. Elemental analyses were measured with a Euro EA-CHNS from HEKAtech.

DTA/TG measurements were performed with the help of a thermal analyzer (TGA/SDTA 851^E, METTLER-TOLEDO). For that purpose about 10 mg of the substance was inserted into a corundum container and heated with a constant rate of 10 K min^{-1} under flowing nitrogen. The thermal decomposition was monitored from 30 °C up to 600 °C. Characteristic points like onset and end temperatures of the thermal effects were taken from the differentiated DTA curve following common procedures using the software delivered with the analyzer. Data for X-ray single crystal structure determination were collected either on a Bruker Apex II CCD diffractometer or with the help of an image plate diffractometer (Stoe IPDS I). Details of the data collections were summarized in the Tables 1 and 2. The structures were solved using direct methods (SHELXS-97) and refined by full-matrix least-squares methods (SHELXL-97). All non-hydrogen atoms were refined with anisotropic displacement parameters. The positions of the hydrogen atoms were located from the Fourier difference map at the final stage of the refinement. They were refined in a riding model with the relative isotropic parameters of the heavy atoms to which they are attached. Crystallographic data were deposited with the Cambridge Crystallographic Data Centre (CCDC) and can be obtained free of charge *via* www.ccdc.cam.ac.uk/data_request/cif, or by emailing data_request@ccdc.cam.ac.uk, or by contacting The Cambridge Crystallographic Data Centre, 12, Union Road, Cambridge CB2 1EZ, UK; fax: +44 1223 336033.

X-Ray powder diffraction investigations were performed with the help of the powder diffractometer STADI P (STOE) using Cu-Kα_1 radiation a flat sample holder or thin walled glass capillaries. The same diffractometer was used for high temperature measurements. For that purpose it was equipped with a capillary furnace and silica capillaries were used for sample preparation.

Computational methods. All calculations concerning the structure and energetics of H_2BDSF_4, H_2BDSCl_4 and the corresponding dianion $BDSCl_4^{2-}$ were performed using the Gaussian03 quantum chemistry program package.[22] Using a correlation consistent basis set of cc-pVDZ quality, we report conventional *ab initio* calculations at the Møller–Plesset 2nd order perturbation theory (MP2) level. Unconstrained geometry optimizations of H_2BDSF_4, H_2BDSCl_4 and its dianion were performed. In general, two conformations should be distinguished. The first conformation corresponds to a "staggered" conformation of the sulfonate groups, in which the –OH moieties are located in an *anti* position. The second conformation can be characterized by a geometry in which the sulfonate groups are oriented "eclipsed" with the –OH moieties in *syn* position on the same side of the aromatic ring. The structural and energetic differences are analyzed.

1,4-Bis(dimethylaminothiocarbonyloxy)-2,3,5,6-tetrafluorobenzene (10). *N*,*N*-Dimethylthiocarbamoylchloride (10.2 g, 82.4 mmol, 3.00 eq.) was added to a suspension of tetrafluorohydroquinone (**9**) (5.00 g, 27.5 mmol, 1.00 eq.) and DABCO (12.3 g, 110 mmol, 4.00 eq.) in DMF (72 ml). The resulting mixture was stirred for 0.5 h at 35 °C and then for 2 h at 80 °C. After cooling to ambient temperature, H_2O (80 ml) was added. The precipitate was filtered off, washed with H_2O, dried in vacuum and purified by column chromatography on SiO_2 [gradient elution from hexane/MTBE 1 : 1 → MTBE, R_f(MTBE) = 0.55] to yield the title compound **10** (7.41 g, 9.79 mmol, 76%) as a colorless solid, mp. 184–185 °C. ^{1}H-NMR (500 MHz, $CDCl_3$): δ = 3.39 (s, 6 H), 3.47 (s, 6 H) ppm. ^{13}C{^{1}H}-NMR (125 MHz, $CDCl_3$): δ = 39.1 (CH_3), 44.1 (CH_3), 129.8–130.1 (m; C–O), 141.4 (dm, ^1J = 249 Hz; C–F), 184.6 (C–O) ppm. ^{19}F{^{1}H}-NMR (470 MHz, $CDCl_3$): δ = −153.87 ppm. IR (ATR): nu(tilde) = 2949 (w), 1549 (m), 1504 (s), 1397 (s), 1261 (s), 1171 (m), 1090 (br, s), 987 (s), 910 (m), 721 (m) cm^{-1}. MS (EI, 70 eV), *m*/*z* (%) = 356 (23) [M$^+$], 88 (100). HRMS: calcd. 356.0276 (for $C_{12}H_{12}F_4N_2O_2S_2$), found 356.0285 [M$^+$]. $C_{12}H_{12}F_4N_2O_2S_2$ (356.36 g mol^{-1}).

1,4-Bis(dimethylaminocarbonylthio)-2,3,5,6-tetrafluorobenzene (11). A suspension of thiocarbamate **10** (7.40 g, 20.8 mmol) in Ph_2O (14 ml) was stirred for 1 h at 200 °C (pre-heated oil bath). After cooling to ambient temperature, the precipitate was filtered off, washed with MeOH (10 ml) and dried in vacuum. The crude product was purified by chromatography on SiO_2 [gradient elution hexane/MTBE 1 : 1 → MTBE → CH_2Cl_2, R_f(hexane/MTBE 1 : 1) = 0.17] to yield the title compound **11** (4.52 g, 12.7 mmol, 61%) as a colorless solid, mp. 232–233 °C. ^{1}H-NMR (500 MHz, $CDCl_3$): δ = 3.04 (br, s, 6H), 3.16 (br, s, 6H) ppm. ^{13}C{^{1}H}-NMR (125 MHz, $CDCl_3$): δ = 37.2 (CH_3), 111.4–111.8 (m, C–S), 147.3 (dm, $^1J_{C\text{–}F}$ = 250 Hz, C–F), 161.8 (C=O) ppm. ^{19}F{^{1}H}-NMR (470 MHz, $CDCl_3$): δ = −131.17 ppm. IR (ATR): nu(tilde) = 2943 (w), 1679 (s), 1468 (s), 1361 (m), 1257 (m), 1247 (m), 1101 (m), 957 (s), 901 (m), 813 (m), 689 (s) cm^{-1}. MS (EI, 70 eV), *m*/*z* (%) = 356 (15) [M$^+$], 72 (100). HRMS: calcd. 356.0276 (for $C_{12}H_{12}F_4N_2O_2S_2$), found 356.0282 [M$^+$]. Anal. calcd. for $C_{12}H_{12}F_4N_2O_2S_2$ (356.36 g mol^{-1}): C 40.44, H 3.39, N 7.86, S 18.00; found: C 40.41, H 3.35, N 7.69, S 17.93.

2,3,5,6-Tetrafluoro-1,4-benzenedisulfonic acid dichloride (12). NCS (2.73 g, 20.5 mmol, 8.10 eq.) and hydrochloric acid (2 mol dm^{-3}, 1.4 ml, 2.8 mmol, 1.1 eq.) were added to a cooled (ice-water bath) suspension of thiocarbamate **11** (900 mg, 2.53 mmol, 1.00 eq.) in MeCN (7.1 ml). The mixture was further stirred at

10–15 °C. After 1.5 h a clear solution should have formed; if not, conc. hydrochloric acid (0.45 ml) was added and the mixture further stirred at 10 °C, until a clear solution had formed. Subsequently, the solution was warmed to ambient temperature and stirred, until again a cloudy precipitation appears (10–15 min). The resulting suspension was further stirred for 0.5 h at 23 °C, then H_2O (20 ml) and MTBE (20 ml) were added. The layers were separated and the aqueous layer was extracted twice with MTBE (2 × 30 ml). The combined organic layers were washed with H_2O (30 ml) and dried ($MgSO_4$). After filtration, the solvent was evaporated and the residue chromatographed [SiO_2, CH_2Cl_2, R_f(MTBE) = 0.72] to give a material (379 mg), which was further purified by recrystallization from $CHCl_3$ to yield the title compound **12** (292 mg, 0.84 mmol, 33%) as a colorless solid, mp. 155 °C. $^{13}C\{^1H\}$-NMR (125 MHz, $CDCl_3$): $\delta = 128.2–128.3$ (m, C–S), 144.0 (dm, $^1J_{C-F} = 273$ Hz, C–F) ppm. $^{19}F\{^1H\}$-NMR (470 MHz, $CDCl_3$): $\delta = -129.79$ ppm. IR (ATR): nu(tilde) = 1479 (s), 1395 (s), 1266 (s), 1246 (m), 1174 (s), 989 (s), 796 (w), 636 (s) cm^{-1}. MS (EI, 70 eV), m/z (%) = 346 (18) [M^+], 311 (70), 247 (36), 148 (100), 117 (38). HRMS: calcd. 345.8551 (for $C_6Cl_2F_4O_4S_2$), found 345.8558 [M^+]. Anal. calcd. for $C_6Cl_2F_4O_4S_2$ (347.09 g mol^{-1}): C 20.76, S 18.48; found C 20.79, S 18.80.

2,3,5,6-Tetrafluoro-1,4-benzenedisulfonic acid dihydrate (7) ($H_2BDSF_4\cdot 2H_2O$). A suspension bissulfonylchloride **12** (65 mg, 0.19 mmol, 1.00 eq.) in H_2O (6.5 ml) was heated to reflux for 16 h. After filtration, all volatile materials were evaporated from the filtrate in vacuum to yield the dihydrate of the title compound **7** (66 mg, 0.19 mmol, 100%) as a colorless solid, mp. 169 °C. $^{13}C\{^1H\}$-NMR (125 MHz, D_2O): $\delta = 123.9–124.0$ (m, C–S), 143.5 (dm, $^1J = 253$ Hz, C–F) ppm. $^{19}F\{^1H\}$-NMR (470 MHz, D_2O): $\delta = -138.5$ ppm. IR (ATR): nu(tilde) = 3190 (br, m), 1688 (br, m), 1464 (s), 1403 (w), 1262 (s), 1179 (br, s), 1035 (s), 973 (s), 624 (s) cm^{-1}. ESI-MS (negative mode), m/z = 309 [M − H^+], 154 [M − $2H^+$]. HR-MS (ESI, negative mode): calcd. 308.9151 (for $C_6HF_4O_6S_2$), found 308.9147 [M − H^+]. $C_6H_2F_4O_6S_2\cdot 2H_2O$ (346.23 g mol^{-1}).

1,4-Dinitro-2,3,5,6-tetrachlorobenzene (14). Oleum (H_2SO_4 with 65% SO_3, 143 g, 72.0 ml, 554 mmol, 24.0 eq.) was added at 0 °C to a mixture of 1,2,4,5-tetrachlorobenzene (**13**) (5.0 g, 23 mmol, 1.0 eq.) and $NaNO_3$ (12.0 g, 139 mmol, 6.0 eq.). The resulting mixture was heated to reflux for 14 h, and then cooled with an ice-bath. Water (100 ml) was carefully added and the mixture poured on ice (500 g). The precipitate was collected by filtration, washed with water (30 ml), dried in vacuum and finally recrystallized from MeOH–$CHCl_3$ (2: 3, 160 ml) to yield the title compound **14** (5.6 g, 19 mmol, 80%) as colorless needles, mp. 228 °C. $^{13}C\{^1H\}$-NMR (125 MHz, $CDCl_3$): $\delta = 126.1$ (C-2), 149.3 (C-1) ppm. IR (ATR): nu(tilde) = 1544 (s), 1393 (m), 1335 (s), 1241 (s), 1241 (m), 1134 (m), 1037 (w), 862 (m), 784 (s), 631 (s) cm^{-1}. MS (EI, 70 eV): m/z (%) = 304 (100) [M^+], 212 (60), 177 (40), 142 (65). HR-MS (EI, 70 eV): calcd. 303.8612 (for $C_6Cl_4N_2O_4$), found 303.8610 [M^+]. Anal. calcd. for $C_6Cl_4N_2O_4$ (305.89 g mol^{-1}): C 23.56, N 9.16; found C 23.47, N 9.11.

Disodium 2,3,5,6-tetrachloro-1,4-benzenedisulfonate monohydrate (15) ($Na_2BDSCl_4\cdot H_2O$). A solution of Na_2SO_3 (8.2 g, 65 mmol, 5.0 eq.) in H_2O (65 ml) was added to a suspension of dinitrotetrachlorobenzene (**14**) (4.0 g, 13 mmol, 1.0 eq.) in 1,4-dioxane (35 ml). The resulting mixture was heated to reflux for 16 h. After cooling to ambient temperature, the solvents were evaporated in vacuum. The solid residue was extracted with H_2O (60 ml) and after filtration again washed with H_2O (30 ml) und finally dried in high vacuum to yield the monohydrate of the title compound **15** (4.7 g, 11 mmol, 83%) as a colorless solid, mp. 132 °C (dec). $^{13}C\{^1H\}$-NMR (125 MHz, D_2O): $\delta = 133.3$ (C-2), 142.4 (C-1) ppm. IR (ATR): nu(tilde) = 3470 (m, br), 1644 (m), 1302 (s), 1251 (m), 1219 (s), 1115 (s), 1045 (s), 701 (m), 665 (m), 626 (s) cm^{-1}. MS (ESI, negative mode): m/z = 395 [M − Na^+], 186 [M − $2Na^+$]. HR-MS (ESI, negative mode): calcd. 394.7788 (for $C_6Cl_4NaO_6S_2$), found 394.7798 [M − Na^+]. Anal. calcd. for $C_6H_2Cl_4Na_2O_7S_2$ (437.99): C 16.45, H 0.46, S 14.64; found C 16.58, H 0.31, S 14.90 ($Na_2BDSCl_4\cdot H_2O$).

2,3,5,6-Tetrachloro-1,4-benzene disulfonic acid trihydrate (8) ($H_2BDSCl_4\cdot 3H_2O$). A solution of sodium salt **15** (1.5 g, 3.4 mmol) in H_2O (100 ml) was submitted through a column (5 cm × 9 cm) of freshly activated, acidic Amberlyst®-15 ion exchange resin (50 g). The eluent (H_2O 300 ml) was collected until pH was neutral. The solvent was evaporated in vacuum and the residue redissolved in H_2O (30 ml). After centrifugation and filtration, the filtrate was again evaporated in vacuum to give the title compound **8** (1.1 g, 2.6 mmol, 75%) as a light yellow solid, mp. 197–199 °C (decomp.). $^{13}C\{^1H\}$-NMR (125 MHz, D_2O): $\delta = 133.2$ (C-2), 142.3 (C-1) ppm. IR (ATR): nu(tilde) = 3124 (s, br), 1667 (s, br), 1306 (s), 1243 (m), 1163 (s), 1101 (s), 1010 (s, br), 703 (m), 664 (m), 646 (m) cm^{-1}. MS (ESI, negative mode): m/z = 373 [M − H^+], 186 [M − $2H^+$]. $C_6H_2Cl_4S_2O_6\cdot 3H_2O$ (430.06 g mol^{-1}).

Zinc(II)(1,4-benzenedisulfonate)*bis*(dimethylformamide) [Zn(BDS)(DMF)$_2$]. A mixture of 19 mg $Zn(OH)_2$ (0.191 mmol), 17 mg $H_2BDS\cdot 2H_2O$ (**4**) (0.062 mmol) and 3 ml DMF were sealed in a glass ampoule. The ampoule was placed in a resistance furnace and heated up to 105 °C within 6 h. After 24 h the furnace was slowly cooled to room temperature within 96 h. The product was obtained as transparent single crystals which were separated from the supernatant liquid by decantation.

Zinc(II)(2,3,5,6-tetrafluorobenzene-1,4-disulfonate)*tetrakis*(dimethylformamide) [Zn(BDSF$_4$)(DMF)$_4$]. A mixture of 18 mg $Zn(OH)_2$ (0.181 mmol), 20 mg $H_2BDSF_4\cdot 2H_2O$ (**7**) (0.062 mmol) and 3 ml DMF were sealed in a glass ampoule. The ampoule was placed in a resistance furnace and heated up to 105 °C within 6 h. After 24 h the furnace was slowly cooled to room temperature within 96 h. The product was obtained as transparent single crystals which were separated from the supernatant liquid by decantation.

Zinc(II)(2,3,5,6-tetrachlorobenzene-1,4-disulfonate)*tetrakis*(dimethylformamide) [Zn(BDSCl$_4$)(DMF)$_4$]. To a solution of 0.05 g $H_2BDSCl_4\cdot 2H_2O$ (**8**) (0.12 mmol) in 3.5 ml DMF 39 mg $Zn(NO_3)_2\cdot 6H_2O$ (0,13 mmol) were added. The reaction mixture was kept at 50 °C for 24 h. When the solution was reduced to 2/3 of its initial volume, the crystallization of colorless crystals starts. After evaporation of further solvent the crystals were collected by suction.

Copper(II)(2,3,5,6-tetrafluorobenzene-1,4-disulfonate) hexahydrate [Cu(H$_2$O)$_6$](BDSF$_4$). $Cu_2(OH)_2(CO_3)$ (33.2 mg, 0.15 mmol) was added at 50 °C in three portions over 2 h to a solution of $H_2BDSF_4\cdot 2H_2O$ (**7**) (106 mg, 0.30 mmol) in H_2O (5 ml). The resulting blue solution was stirred for 16 h at 50 °C, then filtered and cooled to ambient temperature. After a few days in air at room temperature blue crystals grew from the solution. They were collected by suction and dried under ambient conditions.

Copper(II)(2,3,5,6-tetrachlorobenzene-1,4-disulfonate) tetrahydrate [$Cu(BDSCl_4)(H_2O)_4$]. $Cu_2(OH)_2(CO_3)$ (134 mg, 0.60 mmol) was added at 50 °C in three portions over 2 h to a solution of H_2BDSCl_4 (**8**) (100 mg, 0.26 mmol) in H_2O (10 ml). The resulting blue suspension was stirred for 24 h at 50 °C, then diluted with 50 ml H_2O and kept at 50 °C for 10 min. Excess malachite was removed by filtration and the filtrate was cooled to ambient temperature. After a few days in air at room temperature blue crystals grew from the solution. They were collected by suction and dried under ambient conditions.

Acknowledgements

We are grateful to Mr Wolfgang Saak for the collection of X-ray data.

References

1 Recent reviews: (*a*) S. Ma and H.-C. Zhou, *Chem. Commun.*, 2010, **46**, 44–53; (*b*) Z. Wang and S. M. Cohen, *Chem. Soc. Rev.*, 2009, **38**, 1315–1329; (*c*) D. Farrusseng, S. Aguado and C. Pinel, *Angew. Chem.*, 2009, **121**, 7638–7649; D. Farrusseng, S. Aguado and C. Pinel, *Angew. Chem., Int. Ed.*, 2009, **48**, 7502–7513; (*d*) R. A. Fischer and C. Wöll, *Angew. Chem.*, 2008, **120**, 8285–8289; R. A. Fischer and C. Wöll, *Angew. Chem., Int. Ed.*, 2008, **47**, 8164–8168; (*e*) S. Bauer and N. Stock, *Chem. Unserer Zeit*, 2008, **42**, 12–19; (*f*) U. Müller, M. Schubert, F. Teich, H. Puetter, K. Schierle-Arndt and J. Pastre, *J. Mater. Chem.*, 2006, **16**, 626–636; (*g*) S. Kaskel, *Nachr. Chem.*, 2005, **53**, 394–399; (*h*) J. L. C. Rowsell and O. M. Yaghi, *Angew. Chem.*, 2005, **117**, 4748–4758; J. L. C. Rowsell and O. M. Yaghi, *Angew. Chem., Int. Ed.*, 2005, **44**, 4670–4679.

2 (*a*) B. D. Chandler, G. D. Enright, K. A. Udachin, S. Pawsey, J. A. Ripmeester, D. T. Cramb and G. K. H. Shimizu, *Nat. Mater.*, 2008, **7**, 229–235; (*b*) Review: G. K. H. Shimizu, R. Vaidhyanathan and J. M. Taylor, *Chem. Soc. Rev.*, 2009, **38**, 1430–1449.

3 G. P. Panasyuk, L. A. Azarova, G. P. Budova and A. P. Savost'yanov, *Inorg. Mater.*, 2007, **43**, 951–955.

4 A. Mietrach, T. W. T. Muesmann, J. Christoffers and M. S. Wickleder, *Eur. J. Inorg. Chem.*, 2009, 5328–5334.

5 T. W. T. Muesmann, A. Mietrach, J. Christoffers and M. S. Wickleder, *Z. Anorg. Allg. Chem.*, 2010, **636**, 1307–1312.

6 (*a*) Z. Hulvey, E. H. L. Falcao, J. Eckert and A. K. Cheetham, *J. Mater. Chem.*, 2009, **19**, 4307–4309; (*b*) J. H. Yoon, S. B. Choi, Y. J. Oh, M. J. Seo, Y. H. Jhon, T.-B. Lee, D. Kim, S. H. Choi and J. Kim, *Catal. Today*, 2007, **120**, 324–329; (*c*) B. Chen, Y. Yang, F. Zapata, G. Qian, Y. Luo, J. Zhang and E. B. Lobkovsky, *Inorg. Chem.*, 2006, **45**, 8882–8886.

7 M. Y. He, S.-C. Chen, Z.-H. Zhang, K.-L. Huang, F.-H. Yin and Q. Chen, *Inorg. Chim. Acta*, 2009, **362**, 2569–2576.

8 (*a*) P. Satori and G. Bauer, *J. Fluorine Chem.*, 1978, **12**, 203–210; (*b*) See also: P. Satori and G. Bauer, *J. Fluorine Chem.*, 1979, **14**, 201–221; (*c*) P. Satori and H. J. Frohn, *Chem. Ber.*, 1974, **107**, 1195–1206.

9 (*a*) J. N. Harvey, J. Jover, G. C. Lloyd-Jones, J. D. Moseley, P. Murray and J. S. Renny, *Angew. Chem.*, 2009, **121**, 7748–7751; J. N. Harvey, J. Jover, G. C. Lloyd-Jones, J. D. Moseley, P. Murray and J. S. Renny, *Angew. Chem., Int. Ed.*, 2009, **48**, 7612–7615; (*b*) J. S. Albert, D. Aharony, D. Andisik, H. Barthlow, P. R. Bernstein, R. A. Bialecki, R. Dedinas, B. T. Dembofsky, D. Hill, K. Kirkland, G. M. Koether, B. J. Kosmider, C. Ohnmacht, W. Palmer, W. Potts, W. Rumsey, L. Shen, A. Shenvi, S. Sherwood, P. J. Warwick and K. Russell, *J. Med. Chem.*, 2002, **45**, 3972–3983; (*c*) M. S. Raasch, *J. Org. Chem.*, 1979, **44**, 2629–2632.

10 (*a*) M. S. Newman and H. A. Karnes, *J. Org. Chem.*, 1966, **31**, 3980–3984; (*b*) H. Kwart and E. R. Evans, *J. Org. Chem.*, 1966, **31**, 413–419.

11 (*a*) M. Treskow, J. Neudörfl and R. Giernoth, *Eur. J. Org. Chem.*, 2009, 3693–3697. See also: (*b*) M. Barbero, S. Bazzi, S. Cadamuro, S. Dughera, C. Magistris and P. Venturello, *Synlett*, 2010, 1803–1806; (*c*) A. Nishiguchi, K. Maeda and S. Miki, *Synthesis*, 2006, 4131–4134; (*d*) D.-W. Kim, Y. K. Ko and S. H. Kim, *Synthesis*, 1992, 1203–1204.

12 C. L. Diedrich, D. Haase and J. Christoffers, *Synthesis*, 2008, 2199–2210.

13 G. Deacon, J. M. Miller and B. S. F. Taylor, *Aust. J. Chem.*, 1975, **28**, 1499–1509.

14 N. S. Dokunikhin, L. A. Gaeva and G. A. Mezentseva, *Dokl. Akad. Nauk. SSSR*, 1972, **206**, 624–626.

15 G. R. Desiraju, *Chem. Commun.*, 2005, 2995–3001; G. A. Jeffrey, *An Introduction to Hydrogen Bonding*, Oxford University Press, New York 1997, p. 79.

16 L. Brammer, E. A. Bruton and P. Sherwood, *Cryst. Growth Des.*, 2001, **1**, 277–290.

17 C. S. Huber, *Acta Crystallogr., Sect. B: Struct. Crystallogr. Cryst. Chem.*, 1969, **25**, 1140–1149.

18 (*a*) J. J. Wolff, S. F. Nelsen, P. A. Petillo and D. R. Powell, *Chem. Ber.*, 1991, **124**, 1719–1725; (*b*) J. J. Wolff, S. F. Nelsen, D. R. Powell and J. M. Desper, *Chem. Ber.*, 1991, **124**, 1727–1731; (*c*) J. J. Wolff, S. F. Nelsen and D. R. Powell, *J. Org. Chem.*, 1991, **56**, 5908–5911.

19 (*a*) J. Cai, C.-H. Chen, C.-Z. Liao, J.-H. Yao, X.-P. Hu and X.-M. Chen, *J. Chem. Soc., Dalton Trans.*, 2001, 1137–1142; (*b*) G. K. H. Shimizu, G. D. Enright, C. I. Ratcliffe, G. S. Rego, J. L. Reid and J. A. Ripmeester, *Chem. Mater.*, 1998, **10**, 3282–3283.

20 V. Logvinenko, L. Yudanova, N. Yudanov and G. Chekhova, *J. Therm. Anal. Calorim.*, 2003, **74**, 395–399.

21 S. Hickman, L. Peterson, J. Kelley, H.-C. zur Loye, M. D. Smith and D. Rishmawi, 60th Southeast Regional Meeting of the American Chemical Society, 2008, p. 823.

22 M. J. Frisch, G. W. Trucks, H. B. Schlegel, G. E. Scuseria, M. A. Robb, J. R. Cheeseman, J. A. Montgomery, T. Vreven, K. N. Kudin, J. C. Burant, J. M. Millam, S. S. Iyengar, J. Tomasi, V. Barone, B. Mennucci, M. Cossi, G. Scalmani, N. Rega, G. A. Petersson, H. Nakatsuji, M. Hada, M. Ehara, K. Toyota, R. Fukuda, J. Hasegawa, M. Ishida, T. Nakajima, Y. Honda, O. Kitao, H. Nakai, M. Klene, X. Li, J. E. Knox, H. P. Hratchian, J. B. Cross, V. Bakken, C. Adamo, J. Jaramillo, R. Gomperts, R. E. Stratmann, O. Yazyev, A. J. Austin, R. Cammi, C. Pomelli, J. W. Ochterski, P. Y. Ayala, K. Morokuma, G. A. Voth, P. Salvador, J. J. Dannenberg, V. G. Zakrzewski, S. Dapprich, A. D. Daniels, M. C. Strain, O. Farkas, D. K. Malick, A. D. Rabuck, K. Raghavachari, J. B. Foresman, J. V. Ortiz, Q. Cui, A. G. Baboul, S. Clifford, J. Cioslowski, B. B. Stefanov, G. Liu, A. Liashenko, P. Piskorz, I. Komaromi, R. L. Martin, D. J. Fox, T. Keith, M. A. Al-Laham, C. Y. Peng, A. Nanayakkara, M. Challacombe, P. M. W. Gill, B. Johnson, W. Chen, M. W. Wong, C. Gonzalez and J. A. Pople, *Gaussian, Inc., Wallingford CT*, 2004.